Chemical Engineering Journal 164 (2010) 425–431

Contents lists available at ScienceDirect

Chemical Engineering Journal

journal homepage: www.elsevier.com/locate/cej

Relationship between mechanical properties and shape descriptors of granules obtained by fluidized bed wet granulation

Darío I. Téllez-Medina*, Edmond Byrne, John Fitzpatrick, Muammer Catak, Kevin Cronin

Department of Process and Chemical Engineering, University College Cork, College Road, Cork, Ireland

ARTICLE INFO

Article history:
Received 3 July 2009
Received in revised form
12 November 2009
Accepted 27 November 2009

Keywords:
Wet granulation
Coefficient of restitution
Granule strength
Fractal dimension
Lacunarity

ABSTRACT

This paper focuses on two mechanical properties of granules, the coefficient of restitution and the strength, and analyzes their sensitivity to granule geometric parameters. The granules were obtained by fluid bed granulation of glass beads with an aqueous solution of PEG1500. Collisions were arranged between granules, and for granules against two glass plates, the first of them a non-covered plate, whereas the second was a plate covered with a thin film of PEG1500. The coefficient of restitution and the strength were measured for the granules, the former for individual particles also. In the case of individual glass particles the coefficient of restitution was around 0.61 for impacts on the flat glass, and 0.5 on the covered glass; for the granules, this parameter was around 0.44 for both situations and for collisions between granules. Sphericity, lacunarity and fractal dimension of the granule projected area, as well as the granule porosity, were determined. Granules giving the highest values for strength had the largest fractal dimension and the smallest lacunarity values regardless of their sphericity, porosity and coefficient of restitution.

1. Introduction

Fluidized bed technology is employed to achieve granulation of particles with the net agglomeration process being defined by the nature of the inter-particle collisions. Either size enlargement or alternatively attrition and breakage can result from these collisions. In addition, collisions between granules and the walls of the equipment have a significant effect on the evolution of granule size [1]. To understand and predict the outcome of collisions, knowledge of the mechanical properties of the granular material is required [2]. This work focuses on two such properties, the coefficient of restitution and the granule strength. In particular, this work examines their sensitivity to geometric parameters of the granules.

The system under analysis consists of the Würster granulation process based on fluidized bed bottom-spray granulation. The fluidized granules travel up an inner tube and exit out the top into the main chamber, fall down the annular space between the tube and the chamber and then repeat the motion. The granules were assembled from glass beads by addition of PEG1500 into an aqueous solution.

Geometric characteristics, e.g. sphericity, can influence the result of particle collisions, i.e. due to the particle shape and orientation it is possible to obtain different results for particle–particle and wall–particle interactions [3,4]. Another geometric characteristic is the irregularity of particle surface which can be quantified by means of fractal dimension (D_F). Fractal dimension is based on the concepts first proposed by Mandelbrot [5] to characterize natural shapes with mathematical patterns more close to reality than those extracted from Euclidean geometry, and it has been applied to different systems and phenomena to quantitatively describe their morphology [6–10]. The use of fractal dimension as a shape descriptor for granules has been reported by [6,10,11]. Lacunarity (Λ) is a complementary parameter to quantify the heterogeneity in the distribution of void spaces inside a figure or pattern [12]. Comparable to sphericity, D_F and Λ can be determined with image analysis software, by applying the box counting and gliding box methods, respectively [5–14].

2. Experimental

Granules were obtained by fluidized bed wet granulation from 200 g of glass beads (Jencons-PLS, UK) with a mean diameter equal to 268 μm, and 10 g of an aqueous 60% (w/w) dissolution of polyethylene glycol (PEG) 1500 Da (Fluka, Germany). The granulation equipment employed was a Mini-AirPro (Pro-C-epT, Belgium) with the Würster configuration. In Table 1 are resumed the processing conditions. The total processing time was approximately 25 min plus a drying period (1 min) to evaporate the water remaining in the binder liquid making contact with the individual particles.

* Corresponding author.
E-mail address: darioiker@gmail.com (D.I. Téllez-Medina).

1385-8947/$ – see front matter © 2009 Elsevier B.V. All rights reserved.
doi:10.1016/j.cej.2009.11.035

Table 1
Processing conditions used for fluidized bed wet granulation.

Parameter	Value
Air flow ($dm^3\ s^{-1}$)	10.83
Inlet-air temperature (°C)	35
Inlet-air relative humidity (%)	0
Inlet-air pressure (MPa)	0.6
Spray-air pressure (MPa)	0.25
Liquid addition rate ($mg\ s^{-1}$)	6.7

The resultant granules were sieved to have a size interval of 1.2–1.6 mm. Fifteen groups with approximately 20 entities each were taken from randomly chosen portions of the sieved granular material, considering the sample sizes recommended by the statistical software. The granule apparent density (ρ_{app}) was determined for every group by means of a gas pycnometer (Multivolume Pycnometer 1305, Micromeritics, USA) using nitrogen. The nitrogen gets into the spaces between granules but is not capable to penetrate into the granule pores, giving the apparent volume by calculations with differences in gas pressure. This information was used later to calculate granule porosity (ε).

Images of the granules and individual glass beads were captured with the PharmaVision 830 analyzer (Malvern Instruments, UK); this equipment also measures the sphericity of the particles.

A high speed camera (X-Motion Pro, AOS Technologies, Switzerland) at 500 fps was used to determine the coefficient of restitution. It recorded the collisions of granules and individual glass beads against a 15 cm × 15 cm glass plate (4 mm thickness). Each group of particles (with approximately 20 glass beads or granules) were lifted up and then released from a height of 40 cm above the glass plate (Fig. 1) [14]. A free fall from this height supposes an impact velocity close to $2.8\ m\ s^{-1}$, and was selected to reduce the probability of granule breakage when colliding with the plate. The same procedure was developed using a glass plate covered with a uniformly distributed layer of PEG1500 with a thickness around 0.5 mm, but not exceeding this value. The plate was covered with the aqueous solution at the same concentration as that used for the granulation process. The plate was collocated over a horizontal surface, the layer was allowed to solidify for one hour and the thickness of this layer was measured with a vernier caliper. The purpose of using a covered glass plate was to reproduce the surface that probably was present in the final granules.

Using the non-covered glass plate, particles were disposed to collide against the same type of particles in free movement by dividing every group in two parts, releasing one part first against the plate, and the other part approximately 0.5 s later; thus, some particles of the first part were moving up, after the collision against the plate, and collided again but this time with particles of the second part moving down.

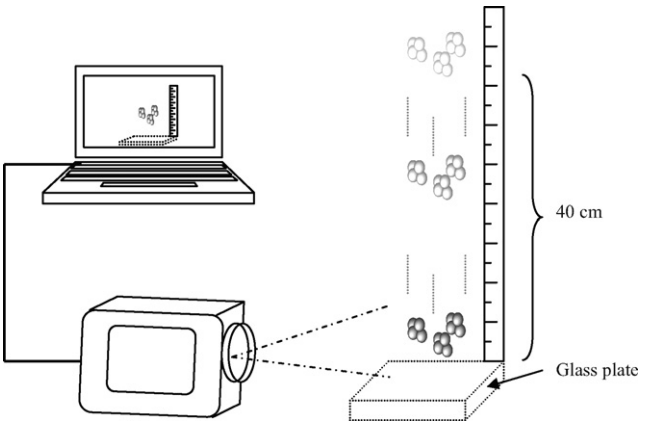

Fig. 1. Diagram of the device used to determine the coefficient of restitution.

Table 2
Characteristics of the materials used for the granules.

Glass beads	PEG1500
Density: 2500 $kg\ m^{-3}$ [a]	Melting point: 43–50 °C [b]
Young's modulus: 63 GPa [a]	Density as solid at 20 °C: 1195 $kg\ m^{-3}$ [b]
Yield stress: 1 GPa [a]	Density as liquid at 55 °C: 1093 $kg\ m^{-3}$ [b]
Poisson's ratio: 0.244 (dimensionless) [a]	Elasticity modulus: 0.2 GPa [a]
Porosity: 0 (dimensionless) [a]	
Mean sphericity: 0.97 (dimensionless) [b]	

[a] Information given by the supplier.
[b] Experimentally determined.

By means of software for dynamic displacement analysis (Pro-Analyst, Xcitex, USA) the ratio of particle velocities before and after the impact was calculated to obtain the coefficient of restitution. Only perpendicular rebounds with the plates or between particles, and without observable breakage and rotation, were taken into account to determine this parameter [2,15]. For collisions between particles, the velocities used were the approaching and separation relative velocities.

A texture analyzer (TA-HD Plus, Stable Micro Systems, UK) was used to measure granule strength as the force needed to fracture the granules by compression, using a P/25 probe operating at $0.1\ mm\ s^{-1}$. For that equipment, such probe is the recommended one to analyze the strength of agglomerates; it consists of an aluminium cylinder with a diameter of 2.5 cm and 2 cm tall. The strength was determined by placing all the granules in each group on the equipment's platen; therefore, one single strength value was obtained per group of granules.

To complete the determination of granule porosity, the true granule density (ρ_{true}) was calculated from binder and solids mass fractions (ψ_b and ψ_s, respectively), which were found by washing two times the granules with distilled water at 85 °C and by evaluating the difference in mass after 2 days inside a desiccator. The following equations were used to calculate porosity:

$$\rho_{true} = \frac{\rho_s \rho_b}{\psi_s \rho_b + \psi_b \rho_s} \quad (1)$$

$$\varepsilon = 1 - \frac{\rho_{app}}{\rho_{true}} \quad (2)$$

In Eq. (1), ρ_s and ρ_b are the solids and binder true density, respectively. The characteristics of the granule constituents are summarized in Table 2.

D_F and Λ were calculated by processing the captured images to analyze the projected area of the particles [7,12,13] with the software ImageJ 1.40g (NIH, USA).

The sequence of measurements described above was performed to the fifteen samples grouped in three batches with five groups each, containing approximately 20 particles (granules or individual glass beads) per group; as illustrated in Fig. 2. In total, five repetitions were done with every collision arrangement (non-covered plate, covered plate, and between particles) for each type of particles (individual glass beads and granules).

Statistical tests were performed with a level of significance $2\alpha = 0.05$ using the software packages SigmaStat 2.0 (Systat Software, USA) and Minitab 14 (Minitab Inc., USA), and consisted of ANOVA sample size, descriptive statistics, one-way and two-way ANOVA, and Grubbs' test.

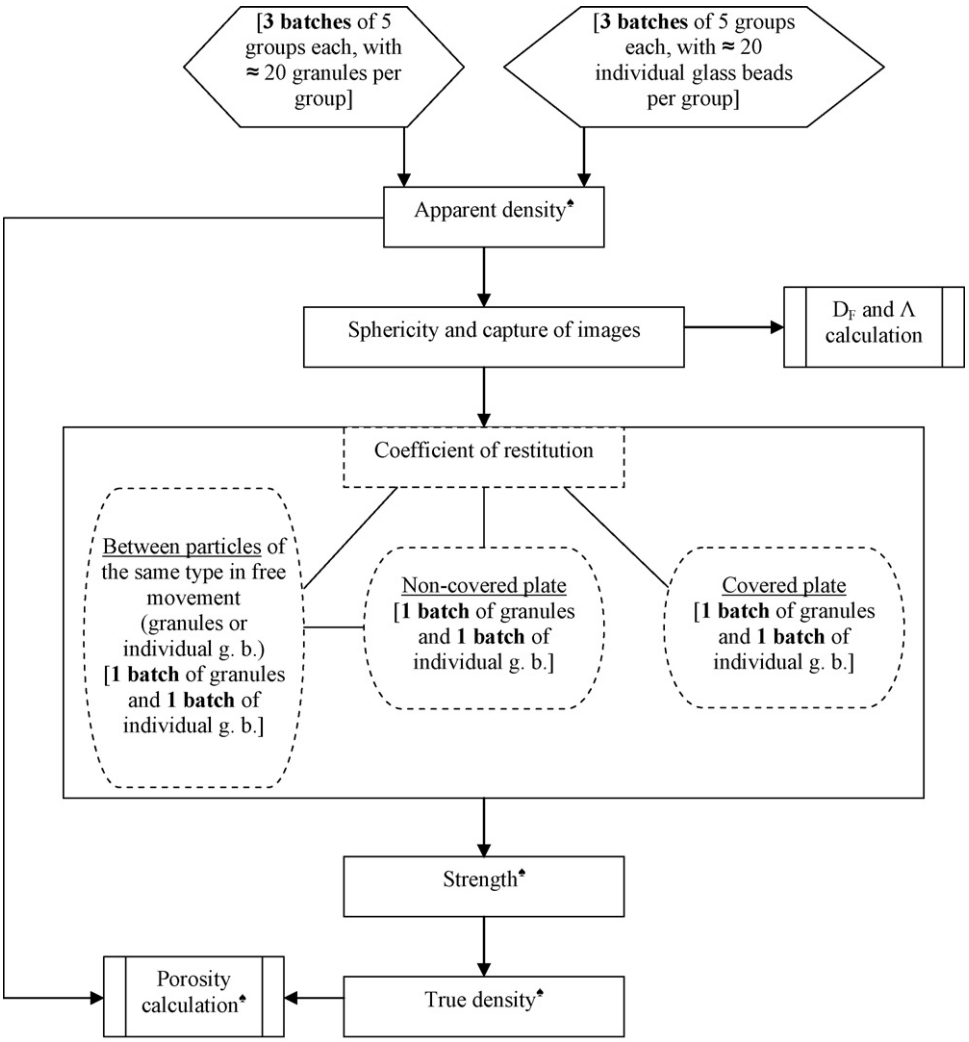

Fig. 2. Sequence of the measurements done to particles. ♠These measurements were carried out for granules only.

3. Results and discussion

3.1. Coefficient of restitution

The coefficient of restitution values for granules and individual glass beads are shown in Fig. 3. The mean values are synopsized in Table 3 and they correspond to the rebounds with the required characteristics detailed in Section 2; therefore, not all the means were calculated from an equal number of data (from 3 up to 8). Fig. 3 and Table 3 also allow comparison of the coefficient of restitution values found for the three different collision arrangements.

For individual glass beads (i.g.b.), the coefficient of restitution had a greater value ($P < 0.001$) when collisions occurred against the non-covered glass plate (Fig. 3a), than for the other arrangements; such value was 0.61 on average. The rigidity of the surface, because of the absence of the polymer, and the fixed position of the plate could explain these results. Nonetheless, a smaller coefficient of restitution was found (0.55 on average) for collisions between individual glass beads than with collisions against the non-covered plate, even though the colliding surfaces consisted of the same material; this could in part be due to the magnitude of the impact velocity (i.e. the relative approaching velocity), approximately $4\,m\,s^{-1}$, higher than in the case of collisions against the plates ($2.8\,m\,s^{-1}$). The glass plate covered with a PEG1500 layer seems to dissipate energy to a greater extent than the non-covered glass [16], resulting in a lower coefficient of restitution of 0.51 on average. The range of coefficient of restitution values suggests a viscoelastic nature for the collisions; this viscoelastic behaviour reduces the amount of energy recovered after the collision [15,16].

For granules, the coefficient of restitution had a statistically non-significant variation ($P \geq 0.466$) when the three different colliding arrangements were used. The mean value for the granules was 0.44, and with all the arrangements granules showed a lower coefficient of restitution than beads ($P < 0.001$ for the three arrangements). This value suggests that collisions had a lower elastic character for granules; and it is possibly due to the internal void spaces, which are not present in the case of i.g.b., and the probable increase in energy dissipation by internal friction during impact [2]. Initially, it was expected a smaller value with the covered plate for both granules and beads, because of the less rigid nature of the polymer in comparison with the glass. Additionally, a lower value was expected for collisions between granules because of the velocity of impact, as in the case of the beads [15].

The void fraction was similar for the granules used in the fifteen repetitions, as it is discussed in Section 3.2; however, an equivalent void fraction in the granule structure, i.e. a similar porosity, could explain the similarity of the coefficient of restitution results when they are compared within the same batch of groups, but not necessary explains the similarity between the different arrangements. The reason of that experimental behaviour could be in the type of

Table 3
Experimental coefficient of restitution.

Particles	Collision arrangement		
	Non-covered plate (2.8 m s^{-1})[a]	Covered plate (2.8 m s^{-1})[a]	Inter-particles (4 m s^{-1})[a]
Individual glass beads	0.61	0.51	0.55
Granules	0.44	0.44	0.44

[a] The representative impact velocity for each arrangement is given in parenthesis.

surfaces making contact during collisions. Probably the granules were covered with PEG1500, thus, there was not a considerable change if the collision took place against another covered (with PEG1500) or non-covered surface. Two complementary examinations to define if this is true could be: (1) the observation of granules with a scanning electron microscope to do a comparison with micrographs captured for covered and non-covered with PEG1500 glass particles; and (2) the determination of the coefficient of restitution against a covered and a non-covered with PEG1500 plate made with other type of material such as steel. Due to the purposes

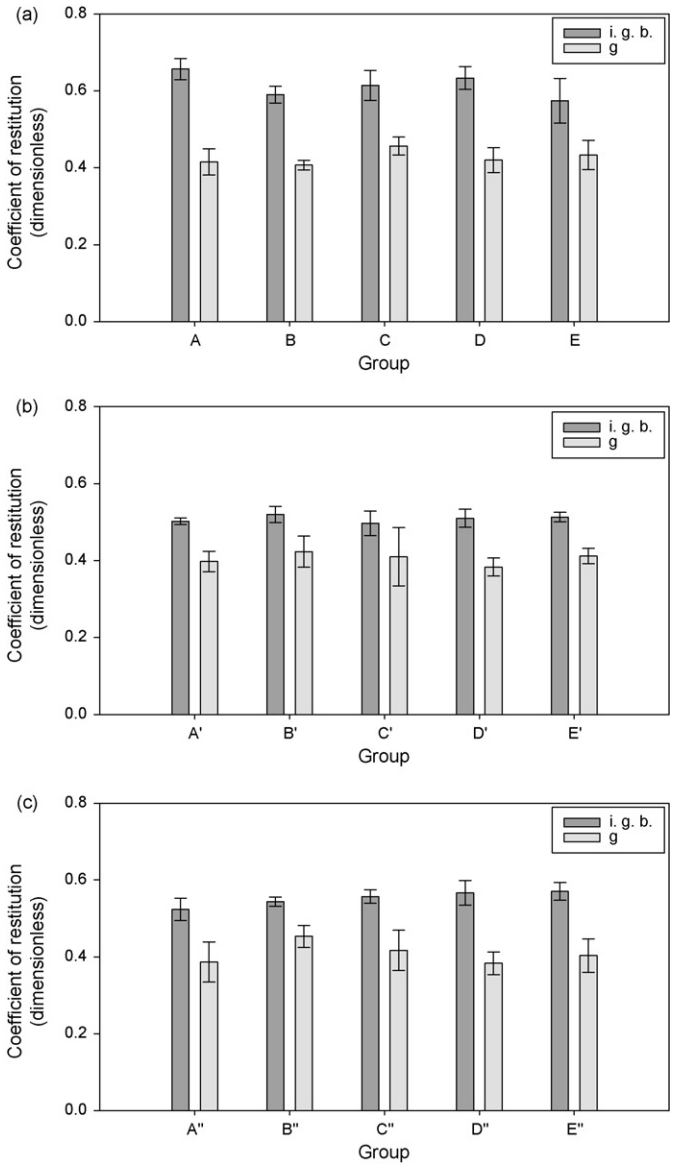

Fig. 3. Mean coefficient of restitution values for individual glass beads (i.g.b.) and glass beads-PEG1500 granules (g); with three different collision arrangements: (a) against a non-covered glass plate; (b) against a covered with PEG1500 glass plate; (c) between particles of the same type in free movement.

established for the present work, namely the exploration of sensitivity to shape descriptors from granule mechanical properties, those suggestions were not carried out.

It was decided to compare measured values of the restitution coefficient with some commonly available literature formulae. There are several reports on the dependence of the coefficient of restitution (e) with respect to the impact velocity (V_i) for collisions of spherical particles against a plane surface, for instance [17]:

$$e = 1.324\left(\frac{Y^5}{\rho_s E_{bp}^{*4}}\right)^{1/8} V_i^{-1/4} \tag{3}$$

where Y is the yield stress, and E_{bp}^* is the representative or effective Young's modulus for the system (glass beads–glass plate, in this case) [15,18]:

$$E^* = \frac{E_s}{1-\nu_s^2} \tag{4}$$

In Eq. (4), E_s is the loading Young's modulus, and ν_s is the Poisson's ratio of the glass beads (cf. Table 1). Alternatively, for collisions between beads with the same mass (m_s) and radius (R_s = 134 μm), the following expressions for inter-spherical collisions could be used [17,18]:

$$e = \left(\frac{6\sqrt{3}}{5}\right)^{1/2}\left[1-\frac{1}{6}\left(\frac{V_y}{V_i}\right)^2\right]^{1/2} \times \left[\frac{V_y/V_i}{(V_y/V_i)+2\sqrt{(6/5)-(1/5)(V_y/V_i)^2}}\right]^{1/4} \tag{5}$$

The term V_y is the yield velocity, i.e. the impact velocity from which plastic deformation occurs, as defined in [15,17,18].

Analyzing granules is more complex. It is necessary to assume a spherical geometry and to take into account porosity by using an equivalent uniform density. Eq. (3) can be used to examine the collision of granules against a flat plate by defining [15]:

$$Y = \frac{\mathrm{d}F}{\mathrm{d}\Delta}\frac{1}{c\pi R_g} \tag{6}$$

$$E_{gp}^* = \frac{3F}{\sqrt{2R_g\Delta^3}} \tag{7}$$

The ratio $\mathrm{d}F/\mathrm{d}\Delta$ is called stiffness and refers to the force (F) per total displacement (Δ) unit, being in the order of 1 N mm^{-1}, obtained by the compression measurements; R_g is the granule radius (0.72 mm), whereas the term c is a constraint factor with a value around three for full plastic deformation [15]. Eq. (7) is used to obtain the effective Young's modulus for the system of granule–glass plate (E_{gp}^*), and this value can be treated to give the effective Young's modulus for the granule–granule collisions (i.e. $E_{gg}^* = 0.5E_{gp}^*$). Table 4 summarizes the input data required for the analytical expressions and gives the predicted values for the coefficient of restitution.

For glass beads against the uncovered plate a coefficient of 0.63 was predicted with an impact velocity of 2.8 m s^{-1}. The value for the collision of two glass beads was 0.67 assuming an approach velocity of 4 m s^{-1}. The former is an excellent agreement with the experimentally found value (0.61) though the latter

Table 4
Theoretical coefficient of restitution.

Property	Collision system			
	Bead–non-covered plate	Bead–bead	Granule–non-covered plate	Granule–granule
Effective Young's modulus (MPa)	6.7×10^4	3.35×10^4	2.2	1.1
Yield stress (MPa)	1×10^3	–	0.14	–
Yield velocity ($m\,s^{-1}$)	–	0.44	–	0.11
Velocity of impact ($m\,s^{-1}$)	2.8	4.0	2.8	4.0
Theoretical coefficient of restitution (dimensionless)	0.63[a]	0.67[b]	0.43[a]	0.48[b]

[a] Eq. (3), using $\rho_s = 2500\,kg\,m^{-3}$.
[b] Eq. (5), using $\rho_{app} = 2443\,kg\,m^{-3}$.

is a serious overestimate (experimental value is 0.55). For the granules the coefficient of restitution values are 0.43 and 0.48 for collisions against the plate ($V_i = 2.8\,m\,s^{-1}$) and between granules ($V_i = 4\,m\,s^{-1}$), respectively. For this case, the average density value must be that of the granule apparent density ($2443\,kg\,m^{-3}$). The measured value for both arrangements is 0.44 which means a very good agreement is reached. However, caution is needed in interpreting the predictions on granule collisions because many assumptions are needed for the calculations and may not be fulfilled in practise.

3.2. Granule porosity, strength and sphericity

In Fig. 4, porosity and sphericity results for the groups of granules used to collide against the non-covered plate (but not against each other) are shown. These groups represent all the batches of granules because the results for the parameters of porosity and sphericity (as for coefficient of restitution), were almost identical ($P > 0.5$); they only exhibited a single difference with respect to the results for strength, D_F and Λ, which is discussed in the following paragraphs. Porosity is relatively invariant amongst the different groups with an average magnitude of 0.01. The average sphericity too is of a similar magnitude across the groups with a value of 0.65; thus granules are not close to a spherical shape.

Fig. 5 contains the results on granule strength. The measured mean granule strength was 1.13 N; primarily the strength value reflects the force needed to deform the polymer bridges. There was one group of granules (group D) within the fifteen that differed significantly ($P < 0.05$) from the rest, as illustrated in Fig. 5. It should be taken into account that strength measurements, as with porosity, were conducted at the same time for all the granules in a group, this is, the strength values do not correspond to individual measurements on granules; therefore, the highest results could be due to only a few of the granules in the group. Fig. 4 shows that the mean sphericity is equivalent in all the groups, which says that differences in strength are not due to sphericity as it would be expected, since the more spherical particles trend to manifest a greater strength [19].

3.3. Fractal dimension (D_F) and lacunarity (Λ)

By means of analysis of the images captured for each particle, it was possible to distinguish that fractal dimension (D_F) had a greater value for the granules than for individual glass beads ($P < 0.001$). Fig. 6 presents the results found for D_F. In many works, D_F is related with the extent of irregularity in an object, that is, in its contour or in its exposed surface [20]. This is the reason for the lower D_F results for individual glass beads. Average fractal dimension for the beads was 1.41 while for the granules was 1.59. The statistically greatest D_F ($P \leq 0.003$) corresponds to the granules with the highest strength. It is necessary to remember that D_F and Λ correspond to (i.e. they were calculated from) the projected area of the particles.

Concerning lacunarity (Λ), as shown in Fig. 7, the values found for individual glass beads are close to zero as expected (0.1 on average). Most of the granules gave Λ values very close to the mean, which equalled 0.4; the exceptions were again the granules with higher strength, whose Λ results are statistically smaller ($P < 0.001$). Structures with low lacunarity values have both a less porous fraction and a more homogeneous geometric distribution (more symmetry) of void spaces [12,21]. Considering this, the individual glass beads presented the mentioned Λ results due to the scarce presence of void spaces in their projected area. The granules of the group with higher strength might have small porosity values; nonetheless, as porosity was similar within the groups of granules,

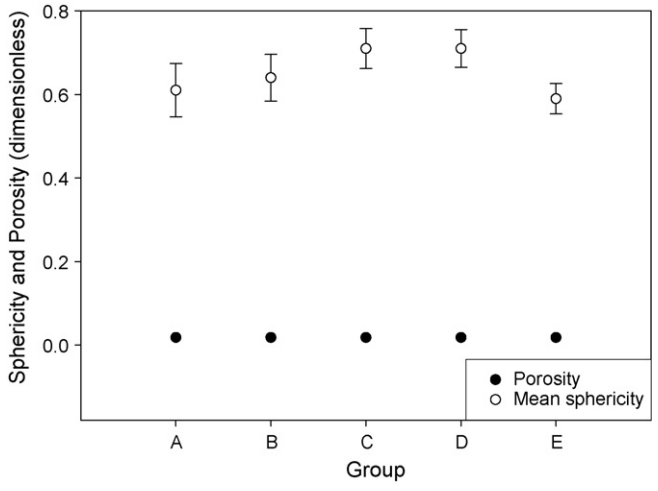

Fig. 4. Porosity and mean sphericity results of the groups of granules (g) employed for Fig. 3(a).

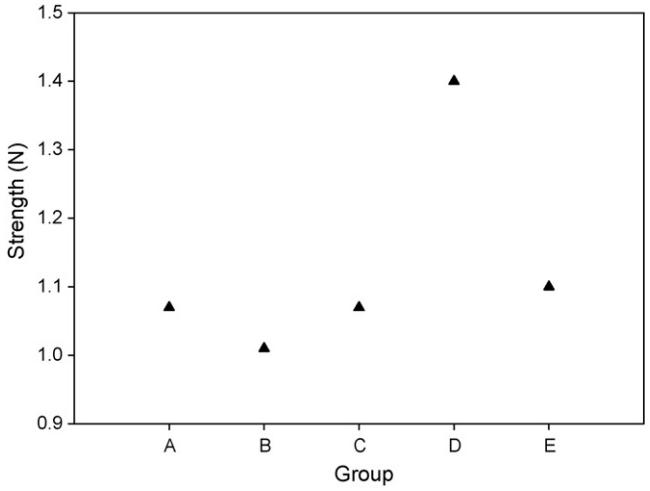

Fig. 5. Strength results for the groups of granules (g) employed for Fig. 3(a).

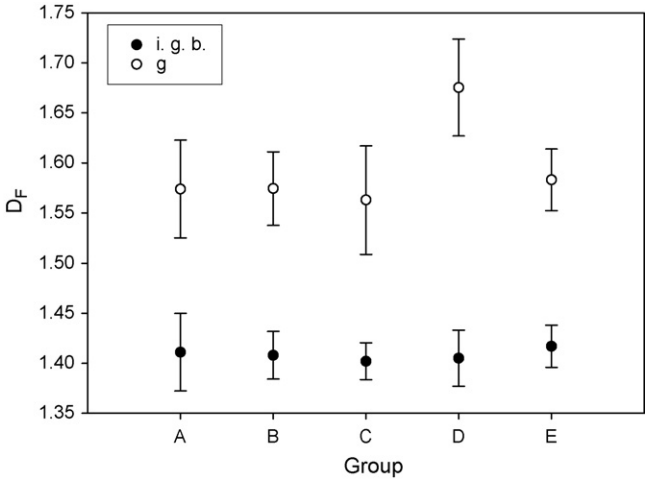

Fig. 6. Fractal dimension (D_F) results with the groups of granules (g) and individual glass beads (i.g.b.) employed for Fig. 3(a).

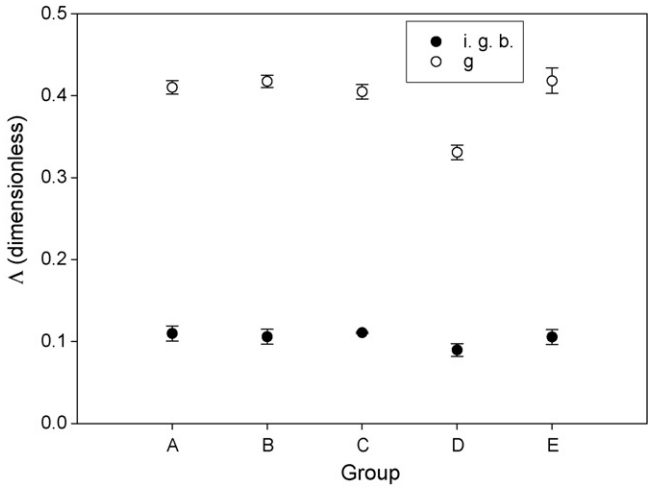

Fig. 7. Lacunarity (Λ) results with the groups of granules (g) and individual glass beads (i.g.b.) employed for Fig. 3(a).

the low Λ values are likely the product of more homogeneity in the granule void-spaces distribution.

3.4. General remarks

It is interesting to note that only in one of the fifteen groups of granules were there entities with a higher strength. As was discussed before, those values could have been originated from a few granules (even from only one) instead of from the entire group. It is not known why there are stronger granules in the total population; that is, the mechanism involved in producing different granule strength levels during granulation is unclear. Obviously, it is also important to find why they are present in such proportion.

For this work some experimental parameters were kept constant between granules (constituent materials, processing conditions, binder-solids mass ratio, size and size distribution) and there was uniformity relating to porosity and sphericity. Possibly, by changing only the size fraction analyzed (different to the 1.2–1.6 mm range), a different amount of pores could be found in the granules with the subsequent variation in lacunarity levels, thereby leading to make more clearly evident the effects of this shape factor on strength and coefficient of restitution. Modifications in binder-solids mass ratio could produce a similar effect on porosity, but also directly affecting the granule mechanical properties.

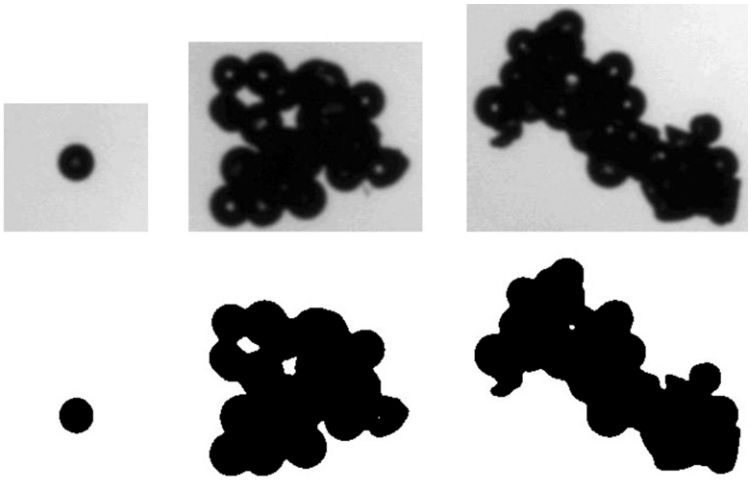

	i)	ii)	iii)
Size (μm):	262*	1355	1604
Porosity (dimensionless)‡:	cf. Table 2*	0.02	0.02
Strength (N)‡:	cf. Table 2*	1.07*	1.40*
Sphericity (dimensionless):	0.98*	0.71	0.65
D_F (dimensionless):	1.42*	1.61*	1.78*
Λ (dimensionless):	0.12*	0.41*	0.34*

Fig. 8. Comparison of representative images of particles, captured with the equipment PharmaVision 830 (Malvern, UK), and their respective projected areas, in the second row, as given by the analysis software ImageJ 1.40g (NIH, USA): (i) glass beads; and glass beads-PEG1500 granules with relatively (ii) low strength, and (iii) high strength. ‡The porosity and strength values correspond to measurements done for the group in which the particle was present; they are not individual results as for the other parameters in the list. *Statistically significant difference ($2\alpha = 0.05$) with respect to the rest of values in the same row.

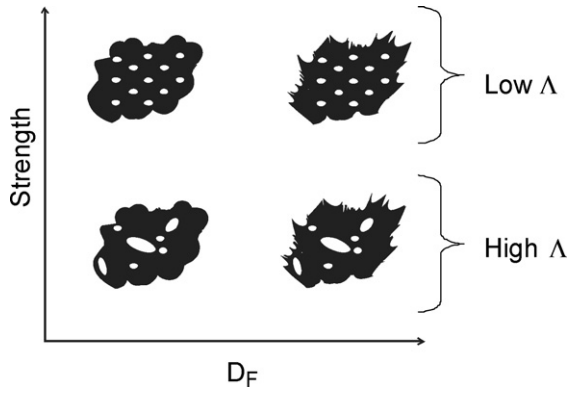

Fig. 9. Hypothetical relationship between granule strength, fractal dimension (D_F), and lacunarity (Λ).

In Fig. 8 there are representative images of granules from groups with relatively low and high strength values; they have a markedly more irregular perimeter than the beads, and the granule from the group with higher strength (Fig. 8 (iii)) seems to have more irregularity. Besides, it is very important to analyze that the granule (ii) belongs to a group with a lower strength although the granule per se has a greater sphericity than granule (iii); therefore, differences in sphericity and strength must be carefully interpreted because sphericity results correspond to individual values for which a statistically significant variation was not found, while the strength is an average value obtained from a group of granules.

Porosity, sphericity and coefficient of restitution are approximately equal across the five groups of granules (A–E). However average fractal dimension D_F and lacunarity, Λ are statistically different for group D compared to the other groups. Another important observation is that all the granules have a void fraction (though minimal) and the mean sphericity differences are negligible. Taking into account that uniformity was set for granule size distribution, it is probable that the higher granule strength for this group can be correlated with D_F and Λ. That is, a granule structure with relatively high contour irregularity (high D_F) and relatively homogeneous distribution of void spaces (low Λ) could exhibit more resistance to breakage by compression (i.e. have high strength), apparently without a direct influence from porosity and sphericity parameters. This idea is presented in Fig. 9. One possible explanation for this association could be that the more irregular the granule shape and the more homogeneity in the distribution of empty spaces inside the granule the greater the extent for dissipation of energy, preventing it from breakage by compression [16,21,22]. Nonetheless, it must be highlighted that it is necessary to evaluate in a systematic way if these hypothetical associations are consistent quantitative correlations, not only for this type of materials but for granule structure in general.

4. Conclusions

The coefficient of restitution for granules produced by fluidized bed wet granulation, made with glass beads and PEG1500, was approximately 0.44 and no differences were found for the three different collision arrangements studied. This is possibly due to the presence of a PEG1500 layer covering the granules. Individual glass beads, in contrast, exhibited a different coefficient of restitution for every collision arrangement, giving on average a higher value for the non-covered plate (0.61), followed by inter-particle collisions (0.55), and those against the covered plate (0.51).

Fractal dimension (D_F) was applied in this work as an index of the contour irregularity, and lacunarity (Λ) as an index of the amount and homogeneity in the distribution of void spaces.

The analysis of mechanical properties (coefficient of restitution and strength) and shape descriptors (sphericity, fractal dimension and lacunarity) for granules with analogous size infers a possible quantitative correlation between strength, contour irregularity and homogeneity in the distribution of the empty spaces inside the granule. The granules with the greatest strength showed also the highest D_F and the lowest Λ results; additionally, this seems to be independent of granule porosity and sphericity, and might occur without an observable change on the coefficient of restitution. The suggested correlations are only hypothetical and must be experimentally and systematically examined.

Acknowledgements

Authors thank to Science Foundation Ireland (SFI) for the financial funding provided. Mr. Darío I. Téllez-Medina thanks also the economic support from the Mexican National Council for Science and Technology (CONACYT).

References

[1] G. Lian, C. Thornton, M.J. Adams, Discrete particle simulation of agglomerate impact coalescence, Chemical Engineering Science 53 (19) (1998) 3381–3391.
[2] J. Fu, M.J. Adams, G.K. Reynolds, A.D. Salman, M.J. Hounslow, Impact deformation and rebound of wet granules, Powder Technology 140 (2004) 248–257.
[3] G.G. Joseph, M.L. Hunt, Oblique particle–wall collisions in a liquid, Journal of Fluid Mechanics 510 (2004) 71–93.
[4] C. Binder, M.A.J. Hartig, W. Peukert, Structural dependent drag force and orientation prediction for small fractal aggregates, Journal of Colloid and Interface Science 331 (2009) 243–250.
[5] B.B. Mandelbrot, The Fractal Geometry of Nature, W.H. Freeman and Company, NY, USA, 1977, pp. 5–19, 25–46.
[6] M. Bellouti, M.M. Alves, J.M. Novais, M. Mota, Flocs vs. granules: differentiation by fractal dimension, Water Research 31 (5) (1997) 1227–1231.
[7] M. Peleg, Fractals and foods, Critical Reviews in Food Science and Nutrition 33 (2) (1993) 149–165.
[8] P.J.J. Chanona, B.L. Alamilla, R.R.R. Farrera, R. Quevedo, J.M. Aguilera, L.G.F. Gutiérrez, Description of the convective air-drying of a food model by means of the fractal theory, Food Science and Technology International 7 (2003) 207–213.
[9] R. Quevedo, G.C. López, J.M. Aguilera, L. Cadoche, Description of food surfaces and microstructural changes using fractal image texture analysis, Journal of Food Engineering 53 (4) (2002) 361–371.
[10] D.K. Kafui, C. Thornton, Fully-3D DEM simulation of fluidised bed granulation using an exploratory surface energy-based spray zone concept, Powder Technology 184 (2008) 177–188.
[11] S.J.R. Simons, Modelling of agglomerating systems: from spheres to fractals, Powder Technology 87 (1996) 29–41.
[12] R.E. Plotnick, R.H. Gardner, W.W. Hargrove, K. Prestegaard, M. Perlmutter, Lacunarity analysis: a general technique for the analysis of spatial patterns, Physical Review E 53 (5) (1996) 5461–5468.
[13] A. Harrison, Fractals in Chemistry, Oxford University Press, Oxford, UK, 1995, pp. 7–34.
[14] H.C. Chun, D. Giménez, S.W. Yoon, Morphology, lacunarity and entropy of intra-aggregate pores: aggregate size and soil management effects, Geoderma 146 (2008) 83–93.
[15] C. Mangwandi, Y.S. Cheong, M.J. Adams, M.J. Hounslow, A.D. Salman, The coefficient of restitution of different representative types of granules, Chemical Engineering Science 62 (2007) (2007) 437–450.
[16] C.Y. Wu, L.Y. Li, C. Thornton, Energy dissipation during normal impact of elastic and elastic–plastic spheres, International Journal of Impact Engineering 32 (2005) 593–604.
[17] C. Thornton, Coefficient of restitution for collinear collisions of elastic-perfectly plastic spheres, Journal of Applied Mechanics 64 (1997) 383–386.
[18] C.Y. Wu, L.Y. Li, C. Thornton, Rebound behaviour of spheres for plastic impacts, International Journal of Impact Engineering 28 (2003) 929–946.
[19] L.M. Tavares, R.P. King, Single-particle fracture under impact loading, International Journal of Mineral Processing 54 (1998) 1–28.
[20] P. Tang, H.K. Chan, J.A. Raper, Validation of computation method to predict aerodynamic diameter of particles with rough surface, Powder Technology 192 (2009) 74–84.
[21] G. Dougherty, A comparison of the texture of computed tomography and projection radiography images of vertebral trabecular bone using fractal signature and lacunarity, Medical Engineering and Physics 23 (2001) 313–321.
[22] A. Carpinteri, M. Paggi, A fractal interpretation of size-scale effects on strength, friction and fracture energy on faults, Chaos, Solitons and Fractals 39 (2009) 540–546.